

AlphaX: eXploring Neural Architectures with Deep Neural Networks and Monte Carlo Tree Search

Linnan Wang*

Department of Computer Science
Brown University
linnan_wang@brown.edu

Yiyang Zhao*

zyyaoiang@gmail.com

Yuu Jinnai

Department of Computer Science
Brown University
yuu_jinnai@brown.edu

Rodrigo Fonseca

Department of Computer Science
Brown University
rfonseca@cs.brown.edu

Abstract

We present AlphaX, a fully automated agent that designs complex neural architectures from scratch. AlphaX explores the exponential search space with a distributed Monte Carlo Tree Search (MCTS) and a Meta-Deep Neural Network (DNN). MCTS intrinsically improves the search efficiency by dynamically balancing the exploration and exploitation at fine-grained states, while Meta-DNN predicts the network accuracy to guide the search, and to provide an estimated reward to speed up the rollout. As the search progresses, AlphaX also generates the training data for Meta-DNN. So, the learning of Meta-DNN is end-to-end. In 14 days with only 16 GPUs (1832 samples), AlphaX found an architecture that reaches the state-of-the-art accuracies on both CIFAR-10(97.18%) and ImageNet(75.5% top-1 and 92.2% top-5). This demonstrates up to 10 \times speedup over the original searching for NASNet that used 500 GPUs in 4 days (20000 samples). In addition, we show the searched architecture improves a variety of vision applications ranging from Neural Style Transfer, to Image Captioning and Object Detection.

1. Introduction

Designing efficient networks currently heavily relies on tremendous heuristics, and the process is extremely laborious. For this reason, Neural Architecture Search (NAS) has sparked a surge of interests. NAS is used to search for networks that meet certain design criteria in a pre-defined search space, and it has succeeded in alleviating the amount of human efforts in the network design [41, 53, 51, 52, 25, 5, 63, 16, 59, 40, 54, 32, 34, 47, 13, 6, 14, 9, 43, 58, 46]. However, the sheer amount of computational power required by

current NAS methods is often prohibitively large (e.g. 10⁴ GPU hours) that motivates us to improve the search efficiency.

In this paper, we present AlphaX, a new DNN design agent aiming at the high search efficiency. The novelty of AlphaX is in a successful marriage of Monte Carlo Tree Search (MCTS) [27, 8] and a Meta-DNN that serves as a predictive model to estimate the accuracy of a sampled architecture. MCTS is a planning algorithm for finding the optimal policy in state-space search problems [8]. The most successful subclass of MCTS is *Upper Confidence bound applied to Trees* (UCT), which introduces a multi-arm bandit algorithm (i.e. UCB1) [4] to a tree search policy [27]. Unlike the existing NAS search algorithms such as Q-Learning, Policy Gradient, Hill Climbing and Evolutionary Algorithms, MCTS dynamically trades off the exploration and exploitation at the finest granularity, i.e. individual architectures, by leveraging the state-level visiting statistics. Meta-DNN has several merits: 1) the prediction skips the expensive training in Monte Carlo rollouts; it quickly estimates a sub-search region rendering by a new node by predicting the average performance for all the children of the new node, so that the search can be guided to a promising region. This is inspired by AlphaGo [49] that utilizes a value predictor and Monte Carlo rollouts to estimate promising states in Go. 2) The prediction also enables us to parallelize the search by decoupling the back-propagation of simulated accuracy and true accuracy. The prediction bias is subsequently offset by the true accuracy once the architecture completes the training. 3) AlphaX generates the new training data for Meta-DNN as training progresses, so the learning of Meta-DNN is end-to-end. In summary, unlike prior works [58, 43], AlphaX is the first to scale up MCTS for NAS, and the first MCTS agent to achieve compelling accuracies on CIFAR-10 and ImageNet.

*Linnan Wang and Yiyang Zhao contributed equally.

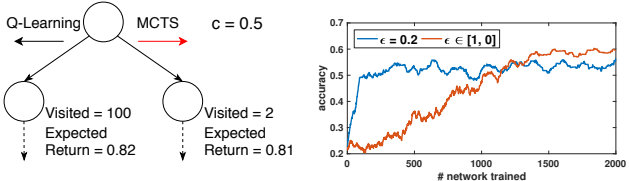


Figure 1: **(left)** the algorithmic behavior without leveraging the visiting statistics; Though we choose QL to illustrate the concept, it is also true for other algorithms such as PG, HC, and EA. **(right)** the importance of exploration to NAS. Better exploration yields a better network. ϵ controls the percentage of random actions (exploration). A large ϵ (orange) yields better networks than a fixed small ϵ (blue) in the limited samples. Please check Appendix Sec.12 for details. Another compelling case is in [58] that π_{CRP} finds a better network than $\pi_{RAVE4NN}$ in a GPU day as $\pi_{RAVE4NN}$ depreciates the exploration in UCT.

2. Related Work

Bayesian Optimization (BO) is a popular method for the hyper-parameter search [24, 50, 57, 26]; It is proven to be an effective black-box optimization technique for small scale problems, e.g. finding good hyper-parameters for Stochastic Gradient Descent (SGD). In a large-scale problem such as NAS, it not only demands a good, sophisticated high-dimensional representation kernel to work, but also requires calculating the inverse of a covariance matrix $\mathcal{O}(n^{2.376})$ that linearly increases with samples (n). These two factors quickly become the key bottleneck in a large scale hyper-parameter search.

Reinforcement Learning (RL): Several RL techniques have been investigated for NAS [5, 63]. Baker et al. proposed a Q-learning agent to design network architectures [5]. In Fig.1, Q-learning seeks to choose an action that exclusively optimizes the best expected return (i.e. accuracy), thus it goes left in the example except for the randomness induced by a stochastic policy (e.g. ϵ -greedy strategy). On the other hand, MCTS chooses to go right because UCB1 explicitly leverages both the expected return and the number of visits to balance the decision. Please check our argument about the importance of exploration and exploitation to NAS in the caption of Fig.1. Zoph et al. built an RNN agent trained with Policy Gradient to design CNN and LSTM [63]. Though found a few not bad networks, directly maximizing expected reward in vanilla Policy Gradient is prone to get trapped in a local optimal [42]. Several techniques have been proposed to mitigate this problem, such as the entropy measures in Soft Actor-Critic[21] and Proximal Policy Optimization [48], adding noise in Deep Deterministic Policy Gradient [29], and the experience replay in Off-Policy Policy Gradient [55]. However, none of these techniques explicitly take the visiting statistics into account in trading-off the exploration and exploitation.

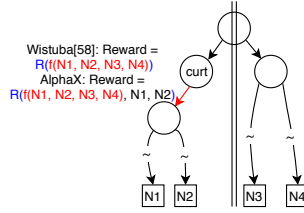


Figure 2: The key difference between AlphaX and [58] in estimating the reward for the action selection. The Gaussian model only utilizes the prediction from a model trained toward entire samples, while AlphaX uses both the prediction and the true accuracies of the node’s children.

Hill Climbing (HC): Elsken et al. proposed a simple hill climbing for NAS [14]. Starting from an architecture, they train every descendent network before moving to the best performing child. Liu et al. deployed a beam search which follows a similar procedure to hill climbing but selects the top-K architectures instead of only the best [33]. HC is akin to the vanilla Policy Gradient tending to trap into a local optimum from which it can never escape, while MCTS demonstrates provable convergence toward the global optimal given enough time[27].

Evolutionary Algorithm (EA): Evolutionary algorithms represent each neural network as a string of genes and search the architecture space by mutation and recombinations [41, 53, 51, 25, 16, 34, 47, 59, 40, 54, 46]. Strings which represent a neural network with top performance are selected to generate child models. The selection process is in lieu of exploitation, and the mutation is to encourage exploration. Still, GA algorithms do not consider the visiting statistics at individual states to inform the decision between the exploitation and exploration.

Monte Carlo Tree Search: DeepArchitect[43] implemented a vanilla MCTS based design agent for NAS, and Wistuba [58] proposed a Gaussian model for predicting rewards for actions. The key difference between AlphaX and the Gaussian prediction model is highlighted in Fig.2. In Fig.2, the ‘red’ action shall be estimated exclusively from its children, N1 and N2. However, the learned model, either meta-DNN in AlphaX or the Gaussian Model in [58], is trained toward the entire data (N1, N2, N3, N4). This implicitly introduces the irrelevant information to distort the estimation. Whereas, the two steps preemptive back-propagation in AlphaX mingles the true accuracy in the estimated reward to improve the estimation. Besides, the Gaussian predictive model also suffers from the scalability issue in BO for calculating the inverse of co-variance matrix, while our meta-DNN is online trainable.

Several approaches have succeeded in speeding up NAS by bypassing the training time for each network architectures with a predictive model for weights.

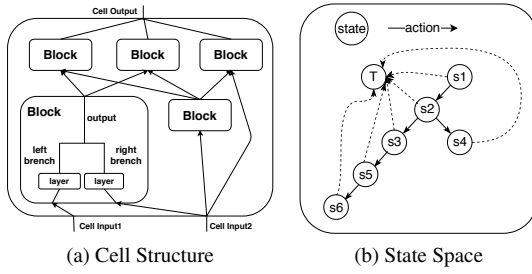


Figure 3: The state and action space of AlphaX.

HyperNet: Because NAS requires training a lot of architectures, eliminating the training time demonstrates a great potential to significantly speedup the search. HyperNet [20] is an approach to use a meta-model to generate DNN weights. SMASH [7] proposes evaluating model architectures with the weights generated from a HyperNet to bypass the actual training. However, the success of these methods is heavily relying on the quality of generated weights.

Knowledge Transfer: Transferring knowledge from previously trained networks to a new network is another approach to reduce the training time for each architecture. Cai et al. [9] integrated Net2Net [11] to RL and successfully reduced the amount of computational resource required. Pham et al. [44] proposed to transfer weights by forcing all child models to share the same weights.

Our method is orthogonal to the purpose of the HyperNet and Knowledge Transfer – our goal is to efficiently search over architectures while these approaches aim to speed up the training time. In fact, our method can be combined with these approaches to reduce the search time.

3. Design Space

The design space of AlphaX is consistent with state space defined in [64] of which the key advantage is at the transferability. That is, the promising architectures found on CIFAR-10 [28] empirically work well on larger image datasets (e.g. ImageNet [12]) too. [64] proposes a network linearly stacked with multiple Cells, and we search for a hierarchical Cell structure as shown in Fig. 3a. There are two types of Cells, Normal Cell (*NCell*) and Reduction Cell (*RCell*). Normal Cell maintains the input and output dimensions with the padding, while Reduction Cell reduces the height and width by half with the striding. The network structure for CIFAR-10 follows "Image→*NCell* (×N)→ *RCell*→ *NCell* (×N)→ *RCell*→ *NCell* (×N)→ softmax", and the network structure for ImageNet follows "Image→3×3 Conv, stride 2→*RCell* (×2)→*NCell* (×N)→ *RCell*→ *NCell* (×N)→ *RCell*→ *NCell* (×N)→ softmax". ×N means repeating N times, and N is empirically set to 6 in experiments. For more information about

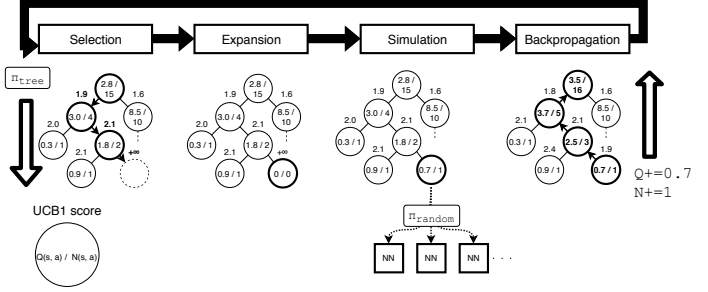


Figure 4: An overview of search procedures in AlphaX.

this design domain, please refer to [64].

4. AlphaX: eXploring Neural Architectures with MCTS and DNNs

4.1. State and Action Space

State Space: A state represents a network architecture, and AlphaX utilizes states (or nodes) to keep track of past trials to inform future decisions. *RCell* and *NCell* are two design units; using two separate state spaces ignores their correlations, so we use one state to represent both structures. A state explicitly captures the internal structures of *RCell* and *NCell*, and their hyper-parameters. We use a sparse data structure such as HashMap to store and reference them. We constrained the state space so that the architectures in the space are manageable within the GPU memory size. Please check Appendix Sec. 8 for more details.

We also introduce a terminal state to allow for multiple actions. All the other states can transit to the terminal state by taking the terminal action (Fig. 3b), and the agent only trains the network, from which it reaches the terminal. Without the terminal state, the agent probes in an undesired progressive manner training shallow networks before going deep. With the terminal state, the agent freely creates new nodes along the path before reaching the terminal. This enables bypassing shallow architectures to directly reach complex architectures.

Action Space: An action morphs the current network architecture, i.e. current state, to transit to the next state. MCTS decides the optimal action, and we will explain it in Section 4.2. Actions we consider are 1) adding a new layer in the left or right branch of *Block_i* in *NCell* or *RCell*, 2) creating a new block in *NCell* and *RCell*, and 3) the terminating. Actions also explicitly specify the connections of *Blocks*. A *Block* has two inputs, which can be either input of current *Cell* or output of existing *Blocks*. The agent prepares each input combinations of a new *Block* in the action set.

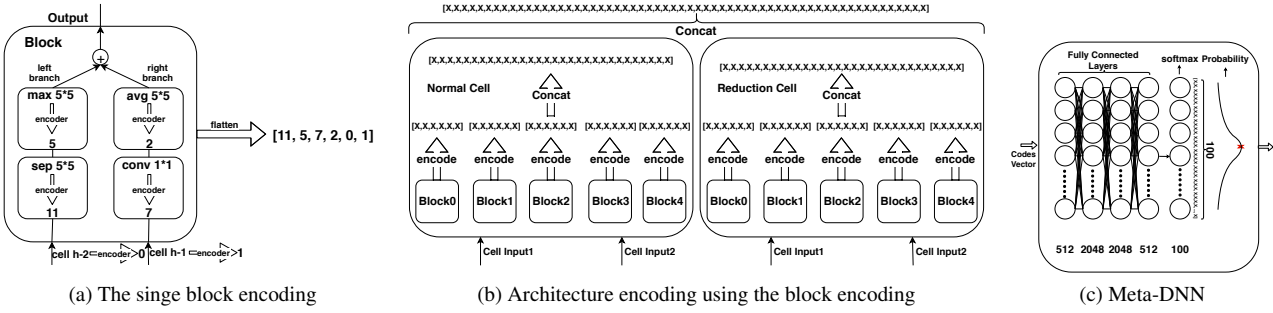


Figure 5: The encoder scheme for network architectures, and the meta-DNN pipeline.

4.2. Search Procedure

In this section, we describe the search procedure of AlphaX. Unlike other search algorithms proposed for NAS, MCTS tracks the visiting statistics at individual nodes to balance the exploration and exploitation at a fine granularity. Each node tracks these two statistics: 1) $N(s, a)$ counts the selection of action a at state s ; 2) $Q(s, a)$ is the expected reward after taking action a at state s , and intuitively $Q(s, a)$ is an estimate of how promising this search direction. Fig.4 demonstrates a typical searching iteration in AlphaX, which consists of *Selection*, *Expansion*, *Meta-DNN assisted Simulation*, and *Backpropagation*. We elucidate each steps as follows.

Selection traverses down the search tree to trace the current most promising search path. It starts from the root and stops till reaching a leaf. At a node, the agent selects actions based on UCB1 [4]:

$$\pi_{tree}(s) = \arg \max_{a \in A} \left(\frac{Q(s, a)}{N(s, a)} + 2c \sqrt{\frac{2 \log N(s)}{N(s, a)}} \right), \quad (1)$$

where $N(s)$ is the number of visits to the state s (i.e. $N(s) = \sum_{a \in A} N(s, a)$), and c is a constant. The first term $(\frac{Q(s, a)}{N(s, a)})$ is the exploitation term estimating the expected accuracy of its descendants. The second term $(2c \sqrt{\frac{2 \log N(s)}{N(s, a)}})$ is the exploration term encouraging less visited nodes. The exploration term dominates $\pi_{tree}(s)$ if $N(s, a)$ is small, and the exploitation term otherwise. As a result, the agent favors the exploration in the beginning until building proper confidences to exploit. c controls the weight of exploration, and it is empirically set to 0.5. We iterate the tree policy to reach a new node.

Expansion adds a new node into the tree. $Q(s, a)$ and $N(s, a)$ are initialized to zeros. $Q(s, a)$ will be updated in the simulation step.

Meta-DNN assisted Simulation randomly samples the descendants of a new node to approximate $Q(s, a)$ of the node with their accuracies. The process is to estimate how

promising the search direction rendered by the new node and its descendants. The simulation starts at the new node. The agent traverses down the tree by taking the uniform-random action until reaching a terminal state, then it dispatches the architecture for training.

The more simulation we roll, the more accurate estimate of this search direction we get. However, we cannot conduct many simulations as the network training is extremely time-consuming. AlphaX adopts a novel hybrid strategy to solve this issue by incorporating a meta-DNN to predict the network accuracy in addition to the actual training. We delay the introduction of meta-DNN to sec.4.3. Specifically, we estimate $q = Q(s, a)$ with

$$Q(s, a) \leftarrow \left(Acc(sim_0(s')) + \frac{1}{k} \sum_{i=1..k} Pred(sim_i(s')) \right) / 2 \quad (2)$$

where $s' = s + a$, and $sim(s')$ represents a simulation starting from state s' . Acc is the actually trained accuracy in the first simulation, and $Pred$ is the predicted accuracy from Meta-DNN in subsequent k simulations. If a search branch renders architectures similar to previously trained good ones, Meta-DNN updates the exploitation term in Eq.1 to increase the likelihood of going this branch.

Backpropagation back-tracks the search path from the new node to the root to update visiting statistics. Please note we discuss the sequential case here, and the backpropagation will be splitted into two parts in the distributed setting (sec.4.4). With the estimated q for the new node, we iteratively back-propagate the information to its ancestral as:

$$Q(s, a) \leftarrow Q(s, a) + q, \quad N(s, a) \leftarrow N(s, a) + 1 \quad (3)$$

$$s \leftarrow parent(s), \quad a \leftarrow \pi_{tree}(s)$$

until it reaches the root node.

4.3. The design of Meta-DNN and its related issues

Meta-DNN is a fully connected network that predicts the network accuracy based on previously trained architectures. The architecture of Meta-DNN is $input \rightarrow 512 \rightarrow 2048 \rightarrow$

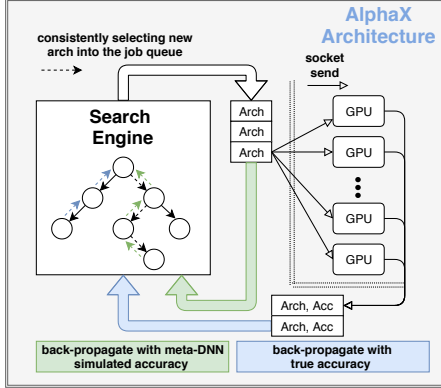


Figure 6: The parallelization scheme of distributed AlphaX. We decouple the original back-propagation into two parts: one uses predicted accuracy (green arrow), while the other uses the true accuracy (blue arrow).

$2048 \rightarrow 512 \rightarrow \text{softmax}$, and each fully connected layers follows a RELU activation. The last softmax outputs a probability distribution over 0~99 categories that represent discretized accuracies in [0%, 99%] at the precision of 1%. The meta-DNN training utilizes previously trained architectures and their accuracies. As AlphaX advances in the searching, it also generates new training data. So, the learning of Meta-DNN is end-to-end. This meta-DNN architecture empirically works well in our case, but we can fine-tune the meta-DNN by observing its performance, either training or validation accuracies, on the collected data.

Meta-DNN takes in a vector that represents an architecture, and we use the following coding scheme to vectorize the architecture: a 6 digits vector codes a *Block* in a *Cell*; the first two digits represent up to two layers in the left branch, while the 3rd and 4th digits represent up to two layers in the right branch. We use the range $1 \sim 12$ to represent 12 different layers (TABLE.3 in Appendix demonstrates the layer types), and we use 0 to pad the vector if a layer is absent. The last two digits represent the input for the left and right branch, respectively. For the input, 0 indicates the input is the output of previous *Cell*, 1 is the previous previous *Cell*, and $i + 2$ indicates the input is the output of *Block*. If a *block* is absent, it is [0,0,0,0,0,0]. Fig.5 demonstrates an example of the proposed encoding scheme. *Block* has 6 digits representing the internal structure and connectivity. A *Cell* has up to 5 *Blocks*, so a vector of 60 digits is sufficient to represent a state that includes both *RCell* and *NCell*.

4.4. Distributed AlphaX

A search iteration of AlphaX involves an actual network training which can take hours to complete. It is imperative to extend AlphaX to work in the distributed setting. Fig.6 demonstrates the distributed AlphaX. There is a master

node exclusively for scheduling the search, while there are multiple clients (GPU) exclusively for training networks. The general procedures on the server side are as follows: 1) The agent follows the normal selection and expansion steps. 2) The simulation in MCTS picks a network $arch_n$ for the actual training, and we push $arch_n$ into a job queue, where $arch_n$ represent the selected network architecture at iteration n , and $rollout_from(arch_n)$ is the node which it started the rollout from to reach $arch_n$. 3) The agent *pre-emptively backpropagates* $\hat{q} \leftarrow \frac{1}{k} \sum_{i=1..k} \text{Pred}(\text{sim}_i(s'))$ based only on predicted accuracies from the Meta-DNN at iteration n .

$$Q(s, a) \leftarrow Q(s, a) + \hat{q}, \quad N(s, a) \leftarrow N(s, a) + 1, \quad (4)$$

$$s \leftarrow \text{parent}(s), \quad a \leftarrow \pi_{\text{tree}}(s).$$

4) The server checks the receive buffer to retrieve a finished job from clients that includes $arch_z$, acc_z . Then the agent starts the second backpropagation to propagate $q \leftarrow \frac{acc_z + \hat{q}}{2}$ (Eq. 2) from the node the rollout started ($s \leftarrow rollout_from(arch_z)$) to replace the backpropagated \hat{q} with q :

$$Q(s, a) \leftarrow Q(s, a) + q - \hat{q}, \quad (5)$$

$$s \leftarrow \text{parent}(s), \quad a \leftarrow \pi_{\text{tree}}(s).$$

A popular approach to parallelize MCTS is by introducing a *virtual loss*, which is a method to avoid making all the processors to traverse the same trajectory by backpropagating a score (i.e. performance of the DNN) of 0 before the rollout finishes and the actual score becomes available to the agent [10, 15, 62, 49]. However, backpropagating a score of 0 can significantly bias the search because the accuracy of the DNN can be close to 1.0, and the variance of the scores among the efficient architectures is often small. Thus, 0 may be significantly smaller than the actual score, biasing the search to avoid the region. To solve this issue, we instead preemptively backpropagate the score \hat{q} predicted by the Meta-DNN which we can expect to be closer to the actual score until the actual training finishes.

The client constantly tries to retrieve a job from the master job queue if it is free. It starts training once it gets the job, then it transmits the finished job back to the server. So, each client is a dedicated trainer. We also consider the fault-tolerance by taking a snapshot of the server's states every few iterations, and AlphaX can resume the searching from the breakpoint using the latest snapshot.

A pseudocode for the whole system is available in Appendix Sec.7.

5. Experiment

This section presents the main experimental results and their discussions: 1) we report the search results on CIFAR-

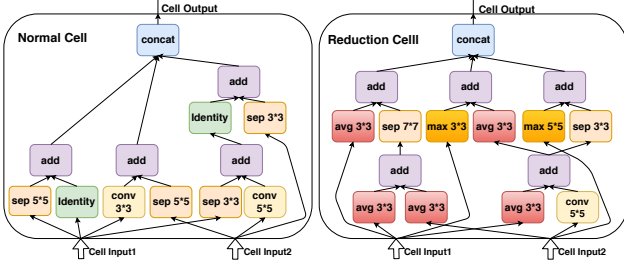


Figure 7: the *RCell* and *NCell* of AlphaX-1 that gives the highest accuracy in the search.

Table 1: The comparisons of our searched architectures to other state-of-the-art results using the same search space defined in [64] on CIFAR-10. In consistent with [64], we observed a well tuned *ScheduleDropPath* significantly affect the final error on both CIFAR-10 and ImageNet, even up to $\pm 1\%$. We report the lowest error with *ScheduleDropPath* tuned to the best of our effort in two months. M is the number of sampled architectures in the search.

model	Search Space	params	err	GPU days	M
DenseNet-BC [23]	human	25.6 M	3.46	N/A	N/A
ResNeXt-29 [60]	human	68.1 M	3.58	N/A	N/A
NASNet-A+cutout [64]	NASNet	3.3M	2.65	2000	20000
NASNet-B [64]	NASNet	2.6M	3.73	2000	20000
NASNet-C [64]	NASNet	3.1M	3.73	2000	20000
AmoebaNet-A+cutout [46]	NASNet	3.2M	3.12	3150	20000
AmoebaNet-B+cutout [46]	NASNet	2.8M	2.50	3150	27000
PNAS [33]	NASNet	3.2M	3.32	225	1160
ENAS [45]	NASNet	4.6M	3.54	0.45	N/A
NAS v3[63]	NAS	7.1M	4.47	22400	12800
NAS v3[63]	NAS	37.4M	3.65	22400	12800
Hier-EA [35]	Hier-EA	15.7M	3.75	300	7000
DARTS+cutout [33]	DARTS	3.3M	2.76	4	N/A
AlphaX-1+cutout (Fig.7)	NASNet	5.1M	2.82	224	1832
AlphaX-2+cutout (Appendix Fig.14)	NASNet	3.5M	3.11	224	1832

10 using 16 NV-1080Ti for 14 days, and our best performing architecture (Fig.7) reaches the comparable accuracy (97.18%) to other state-of-the-art results using the same search space (97.5% \sim 95.53%) on CIFAR-10 with only 224 GPU days. This demonstrates 10x efficiency improvement over the original NAS [64]. Then we use the same architecture for the ImageNet training, and it reaches 92.2% top-5 and 75.5% top-1 beating other state-of-the-art results (top-5 72.5% \sim 75.1% and top-1 91% \sim 92%) in the mobile setting ¹. 2) We exam the performance of meta-DNN, and it demonstrates an average of 1.93% prediction error in the progress of search. 3) We found hyper-parameters such as *ScheduleDropPath* significantly affects the last 1% accuracy ². To eliminate these irrelevant factors in evaluating the search efficiency of proposed method, we design a set of

¹please check [64] for the details of mobile setting.

²This observation is consistent with [64]

Table 2: The error rate (%) comparisons of our best-performing architecture to other state-of-the-art results on ImageNet. The network setup follows the mobile setting defined in [64] with the input image of 224×224 . Multi-adds represents the number of composite multiply-accumulate operations for an image.

model	multi-adds	params	top1/top5 err
ShuffleNet (2x) [39]	569M	6.6 M	30.2/10.1
MobileNet-v1 [22]	524M	4.2 M	29.4/10.5
NASNet-A [64]	564M	5.3M	26.0/8.4
NASNet-B [64]	488M	5.3M	27.2/8.7
NASNet-C [64]	558M	4.9M	27.5/9.0
AmoebaNet-A [46]	555M	5.1M	25.5/8.0
AmoebaNet-B [46]	555M	5.3M	26.0/8.5
AmoebaNet-C [46]	535M	5.1M	24.9/7.9
PNAS [33]	588M	5.1M	25.8/8.1
DARTS [36]	574M	4.7M	26.7/8.7
AlphaX-1	647M	7.2M	24.5/7.8

controlled experiments on a simplified small-scale design domain. Results from 10 independent trials demonstrate that MCTS find the best architecture drastically faster than Hill Climbing, Random Search, Q-Learning, and Meta-DNN further improve the search. 3) Finally, we show that a variety of CV systems, including Neural Style Transfer, Object Detection and Image Captioning, can benefit from NAS by simply replacing the original CNN component with the search optimized one.

5.1. Evaluations of Searched Architectures

Experiment setup: An anonymized reference implementation of AlphaX for the reviewers can be found at [?]. For the details of experimental setup, please check at Appendix Sec.10.

Comparisons to State-of-the-Art Results: AlphaX ran autonomously for 14 days, sampled 1832 networks, from which we select AlphaX-1 and AlphaX-2. AlphaX-1 gives the best accuracy after fine-tuning additional 530 epochs, while AlphaX-2 gives the second best accuracy with 32% fewer parameters than AlphaX-1. Fig.7 demonstrates the architecture of AlphaX-1, and the architecture of AlphaX-2 is at Appendix Fig.14.

Table.1 and Table.2 summarize state-of-the-art results on CIFAR10 and ImageNet. Notably, AlphaX-1 is on par with other state-of-the-art accuracies [64, 46, 45, 33] using approximately 10 times fewer samples(M) and GPU days in the search; the same architecture also gives the best ImageNet accuracy in the mobile setting. We believe ENAS, NASNet, PNAS, and AmoebaNet are fair to compare in speed for using the same search domain. Though ENAS is significantly faster than AlphaX, their approach is orthogonal to us: we focus on the search efficiency, while they focus on reducing the network training time using the parameter sharing (i.e. Transfer Learning). AlphaX can be

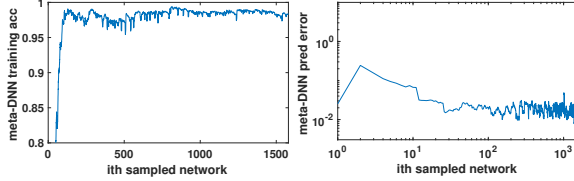


Figure 8: The training accuracy and the average prediction error of meta-DNN in the progress of search for data in Table.1. Before training a new i th sampled network, we estimate its accuracy with the meta-DNN trained toward $[1, i - 1]$ samples. The prediction error is the mean square error between the actual and the estimated accuracy.

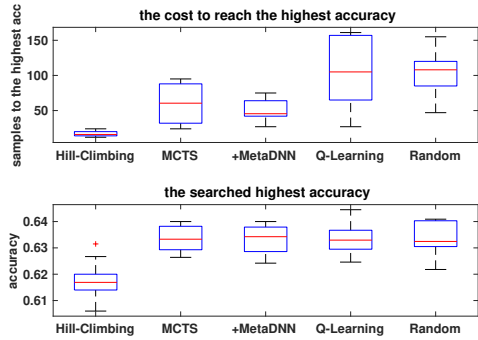


Figure 9: Efficiency evaluations of different search algorithms on a simplified search space. +MetaDNN means MCTS with meta-DNN. The boxplot results from 10 complete search trials. The top boxplot demonstrates the number of samples that each algorithm take to reach the best performing network. The bottom boxplot demonstrates MCTS, Q-Learning and Random Search reach the same best performing network in the search space, while Hill Climbing traps in a local optimal.

further improved by Transfer Learning to drastically reduce the training time on clients. AmoebaNet presents the best error (2.5%). It is likely AmoebaNet sampled 27000 architectures, while we only sampled 1832 due to the limited computing resources. However, both accuracies only differ at 0.0032, which is too small to confidently conclude the cause is from the architecture. In fact, other hyperparameters such as *ScheduleDropPath* in the fine-tuning stage significantly impact the final 1% of accuracy [64]. The speed of PNAS is comparable to AlphaX; but PNAS tends to trap in a local optimal due to the nature of hill-climbing. The effect isn't obvious as the search space of NASNet is so vast, even a sub-optimal architecture still delivers a competitive accuracy. More detailed comparison of hill-climbing is available at 5.3. Though NAS, DARTS and Hier-EA utilize different search spaces, our final accuracy is also comparable to them.

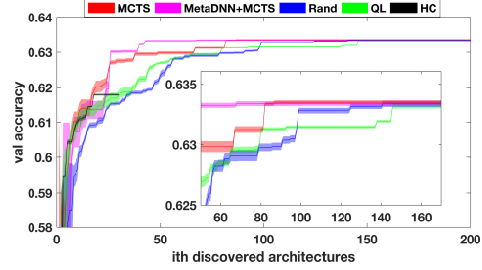


Figure 10: Accuracy progression of the search algorithms in Fig.9. We plot the mean and 3σ range of 10 trials.

5.2. Justification of the Meta-DNN Design

To monitor the performance of meta-DNN, we track both its prediction error and training accuracy in the progress of search. The training accuracy measures how well the meta-DNN learns the already trained architectures, while the prediction error measures how well the meta-DNN generalizes to new architectures. Fig.8 demonstrates both metrics. The training accuracy quickly converges to 98%, and stabilize there. Also, the prediction error quickly reduces down to 2%. Though we agree with other techniques, such as ensemble methods or the RNN based predictor, can be good potential alternatives, the data indicate the current meta-DNN design empirically works well in the search.

5.3. Algorithm Evaluations

Comparing speed on a simplified search space: The NASNet search space is enormous, and each NASNet training lasts over 8 hours. Therefore, it is infeasible for us to perform an exhaustive search. The data collected from the *1 time* partial exploration of search space in Table.1 also mislead us in the quantitative and qualitative evaluations of search algorithms. This motivates us to simplify the search space so that we can conduct several complete searches to rigorously compare the algorithmic efficiency. Appendix Sec.9 demonstrates the details of experiment setup and the simplified search domain. In general, the simplified search domain contains up to 200 architectures, and each architecture follows the design of VGG but up to 3 layers.

Search algorithms evaluations: We compare MCTS against Q-Learning (QL), Hill Climbing (HC) and Random Search (RS) on the simplified search space. We choose these algorithms as they are both widely used in NAS [5, 32, 14, 19], and representing a diverse focus of exploration and exploitation. RS focuses on exploring, and HC focuses on exploiting. QL falls between the two, so does other search algorithms such as Policy Gradient and Genetic Algorithms. Each algorithm searches on the simplified space, and we terminate the search once it finishes ex-

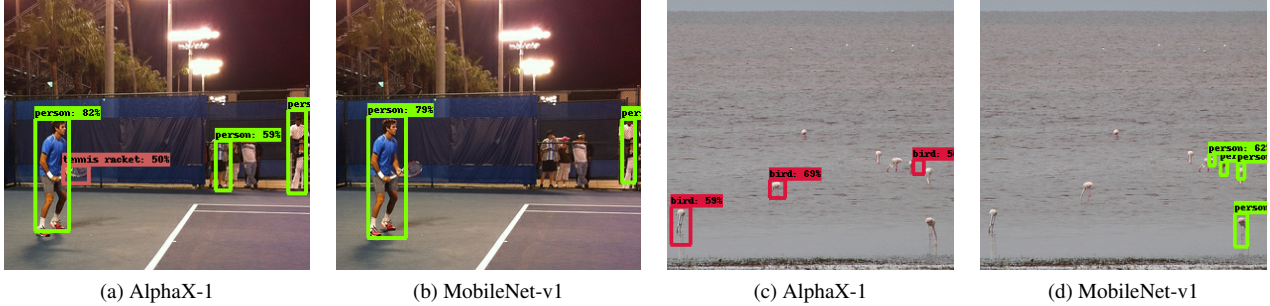


Figure 11: *Object Detection*: the object detection system is more precise with AlphaX-1 than MobileNet.



Figure 12: *Neural Style Transfer*: AlphaX-1 is better than VGG in capturing the style with sophisticated details and textures.

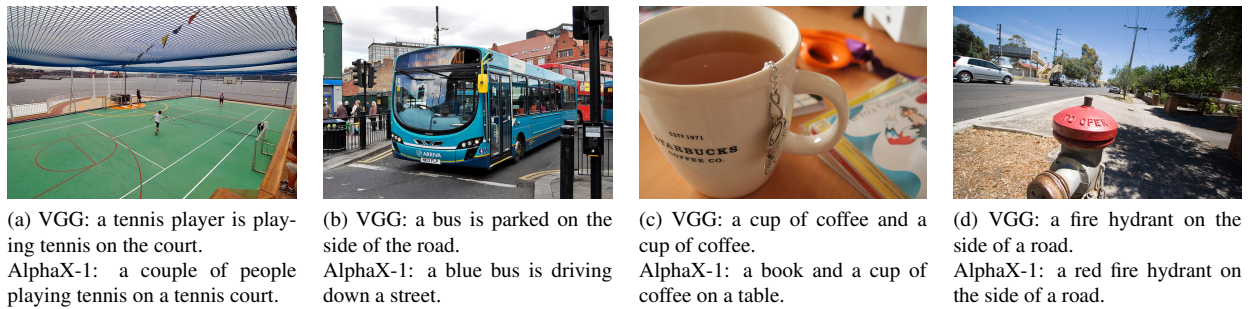


Figure 13: *Image Captioning*: AlphaX-1 captures more details than VGG in the captions.

ploring all the architectures ³. This is defined as a trail of search. We conduct 10 trials for each algorithm. Both Fig.9 and Fig.10 demonstrate MCTS is significantly faster than QL and RS. Though HC is the fastest, the top accuracy difference in Fig.9 (bottom) suggests HC can easily trap into a local optimal. Interestingly, the inter-quartile range of QL is longer than RS because QL quickly converges to a sub-optimal, spending a huge time to escape. This is consistent with Fig.10 that QL converges faster than RS before first 50th samples. In contrast, MCTS keeps track of visiting statistics so that it can quickly escape from a bad search direction. For example, meta-DNN+MCTS is slower than QL and HC in the first few samples, but it finds the global optimal much quicker than QL and HC. Therefore, it is the fastest in finding the global optimal. Both Fig.9 and Fig.10 suggest meta-DNN positively contributes to the search.

³please note HC can easily trap in a local optimal, and we terminate it once it steps into an infinity loop.

5.4. Improved Features for Vision Models

CNN is a common component for Computer Vision (CV) models. Here, we demonstrate NAS can improve a variety of Computer Vision (CV) models simply by replacing the CNN. Please check the Appendix Sec.11 for the experiment setup.

Object detection: We used SSD [37] object detection model, and its TensorFlow implementation is at [3]. By replacing the MobileNet-v1 with AlphaX-1, the mAP (mini-val) increases from 20.1% to 23.7% at the 300×300 resolution. Fig.11 presents examples for qualitative evaluations.

Neural style transfer: [17] suggests deep layers are better than shallow layers at the style reconstruction. As a result, a deep network (AlphaX-1) is better than a shallow network (VGG) in capturing the rich details and textures of a sophisticated style image (Fig.12). Both results are tuned to our best, and the original implementation is at [2].

Image captioning: we replace the VGG with AlphaX-

1 in the model of show attend and tell [61] based on the implementation at [1]. On the 2014 MSCOCO-val dataset, AlphaX-1 achieves 71.7 RELU-1, 52.8 RELU-2, 40.1 RELU-3 and 28.7 RELU-4, respectively. This outperforms VGG in all four RELU $1 \sim 4$.

6. Conclusion

In this paper, we present a new MCTS based design agent for Neural Architecture Search. The agent demonstrates superior search efficiency over a variety of existing search algorithms. In addition, we demonstrate that the searched architecture can improve a variety of CV models.

References

- [1] Tensorflow implementation of image captioning. https://github.com/DeepRNN/image_captioning. 9
- [2] Tensorflow implementation of neural style transfer. <https://github.com/anishathalye/neural-style>. 8
- [3] Tensorflow implementation of single shot multibox detector. https://github.com/tensorflow/models/blob/master/research/object_detection/g3doc/detection_model_zoo.md. 8
- [4] P. Auer, N. Cesa-Bianchi, and P. Fischer. Finite-time analysis of the multiarmed bandit problem. *Machine learning*, 47(2-3):235–256, 2002. 1, 4
- [5] B. Baker, O. Gupta, N. Naik, and R. Raskar. Designing Neural Network Architectures using Reinforcement Learning. pages 1–18, 2016. 1, 2, 7, 14
- [6] A. Brock, T. Lim, J. M. Ritchie, and N. Weston. SMASH: One-Shot Model Architecture Search through HyperNetworks. 2017. 1
- [7] A. Brock, T. Lim, J. M. Ritchie, and N. Weston. Smash: one-shot model architecture search through hypernetworks. *arXiv preprint arXiv:1708.05344*, 2017. 3
- [8] C. B. Browne, E. Powley, D. Whitehouse, S. M. Lucas, P. I. Cowling, P. Rohlfshagen, S. Tavener, D. Perez, S. Samothrakis, and S. Colton. A survey of monte carlo tree search methods. *IEEE Transactions on Computational Intelligence and AI in games*, 4(1):1–43, 2012. 1
- [9] H. Cai, T. Chen, W. Zhang, Y. Yu, and J. Wang. Efficient architecture search by network transformation. *arXiv preprint arXiv:1707.04873*, 2017. 1, 3
- [10] G. M.-B. Chaslot, M. H. Winands, and H. J. van Den Herik. Parallel monte-carlo tree search. In *International Conference on Computers and Games*, pages 60–71. Springer, 2008. 5
- [11] T. Chen, I. Goodfellow, and J. Shlens. Net2net: Accelerating learning via knowledge transfer. *arXiv preprint arXiv:1511.05641*, 2015. 3
- [12] J. Deng, W. Dong, R. Socher, L.-J. Li, K. Li, and L. Fei-Fei. Imagenet: A large-scale hierarchical image database. In *Computer Vision and Pattern Recognition, 2009. CVPR 2009. IEEE Conference on*, pages 248–255. IEEE, 2009. 3
- [13] T. Elsken, J.-H. Metzen, and F. Hutter. Simple And Efficient Architecture Search for Convolutional Neural Networks. pages 1–14, 2017. 1
- [14] T. Elsken, J.-H. Metzen, and F. Hutter. Simple and efficient architecture search for convolutional neural networks. *arXiv preprint arXiv:1711.04528*, 2017. 1, 2, 7
- [15] M. Enzenberger, M. Muller, B. Arneson, and R. Segal. Fuegoan open-source framework for board games and go engine based on monte carlo tree search. *IEEE Transactions on Computational Intelligence and AI in Games*, 2(4):259–270, 2010. 5
- [16] C. Fernando, D. Banarse, M. Reynolds, F. Besse, D. Pfau, M. Jaderberg, M. Lanctot, and D. Wierstra. Convolution by evolution: Differentiable pattern producing networks. In *Proceedings of the Genetic and Evolutionary Computation Conference 2016*, pages 109–116. ACM, 2016. 1, 2
- [17] L. A. Gatys, A. S. Ecker, and M. Bethge. A neural algorithm of artistic style. *arXiv preprint arXiv:1508.06576*, 2015. 8
- [18] L. A. Gatys, A. S. Ecker, and M. Bethge. A neural algorithm of artistic style. *CoRR*, abs/1508.06576, 2015. 14
- [19] K. Greff, R. K. Srivastava, J. Koutník, B. R. Steunebrink, and J. Schmidhuber. Lstm: A search space odyssey. *IEEE transactions on neural networks and learning systems*, 28(10):2222–2232, 2017. 7
- [20] D. Ha, A. Dai, and Q. V. Le. Hypernetworks. *arXiv preprint arXiv:1609.09106*, 2016. 3
- [21] T. Haarnoja, A. Zhou, P. Abbeel, and S. Levine. Soft actor-critic: Off-policy maximum entropy deep reinforcement learning with a stochastic actor. *arXiv preprint arXiv:1801.01290*, 2018. 2
- [22] A. G. Howard, M. Zhu, B. Chen, D. Kalenichenko, W. Wang, T. Weyand, M. Andreetto, and H. Adam. Mobilenets: Efficient convolutional neural networks for mobile vision applications. *arXiv preprint arXiv:1704.04861*, 2017. 6
- [23] G. Huang, Z. Liu, L. Van Der Maaten, and K. Q. Weinberger. Densely connected convolutional networks. In *CVPR*, volume 1, page 3, 2017. 6
- [24] F. Hutter, H. H. Hoos, and K. Leyton-Brown. Sequential model-based optimization for general algorithm configuration. In *International Conference on Learning and Intelligent Optimization*, pages 507–523. Springer, 2011. 2
- [25] R. Jozefowicz, W. Zaremba, and I. Sutskever. An empirical exploration of recurrent network architectures. In *International Conference on Machine Learning*, pages 2342–2350, 2015. 1, 2
- [26] K. Kandasamy, J. Schneider, and B. Póczos. High dimensional bayesian optimisation and bandits via additive models. In *International Conference on Machine Learning*, pages 295–304, 2015. 2
- [27] L. Kocsis and C. Szepesvári. Bandit based monte-carlo planning. In *European conference on machine learning*, pages 282–293. Springer, 2006. 1, 2
- [28] A. Krizhevsky and G. Hinton. Learning multiple layers of features from tiny images. 2009. 3
- [29] T. P. Lillicrap, J. J. Hunt, A. Pritzel, N. Heess, T. Erez, Y. Tassa, D. Silver, and D. Wierstra. Continuous control with deep reinforcement learning. *arXiv preprint arXiv:1509.02971*, 2015. 2
- [30] T. Lin, M. Maire, S. J. Belongie, L. D. Bourdev, R. B. Girshick, J. Hays, P. Perona, D. Ramanan, P. Dollár, and

C. L. Zitnick. Microsoft COCO: common objects in context. *CoRR*, abs/1405.0312, 2014. [13](#), [14](#)

[31] T. Lin, M. Maire, S. J. Belongie, L. D. Bourdev, R. B. Girshick, J. Hays, P. Perona, D. Ramanan, P. Dollár, and C. L. Zitnick. Microsoft COCO: common objects in context. *CoRR*, abs/1405.0312, 2014. [13](#)

[32] C. Liu, B. Zoph, J. Shlens, W. Hua, L.-J. Li, L. Fei-Fei, A. Yuille, J. Huang, and K. Murphy. Progressive Neural Architecture Search. 2017. [1](#), [7](#)

[33] C. Liu, B. Zoph, J. Shlens, W. Hua, L.-J. Li, L. Fei-Fei, A. Yuille, J. Huang, and K. Murphy. Progressive neural architecture search. *arXiv preprint arXiv:1712.00559*, 2017. [2](#), [6](#)

[34] H. Liu, K. Simonyan, O. Vinyals, C. Fernando, and K. Kavukcuoglu. Hierarchical Representations for Efficient Architecture Search. pages 1–13, 2017. [1](#), [2](#)

[35] H. Liu, K. Simonyan, O. Vinyals, C. Fernando, and K. Kavukcuoglu. Hierarchical representations for efficient architecture search. *arXiv preprint arXiv:1711.00436*, 2017. [6](#)

[36] H. Liu, K. Simonyan, and Y. Yang. Darts: Differentiable architecture search. *arXiv preprint arXiv:1806.09055*, 2018. [6](#)

[37] W. Liu, D. Anguelov, D. Erhan, C. Szegedy, S. Reed, C.-Y. Fu, and A. C. Berg. Ssd: Single shot multibox detector. In *European conference on computer vision*, pages 21–37. Springer, 2016. [8](#), [13](#)

[38] I. Loshchilov and F. Hutter. Sgdr: Stochastic gradient descent with warm restarts. *arXiv preprint arXiv:1608.03983*, 2017. [13](#)

[39] N. Ma, X. Zhang, H.-T. Zheng, and J. Sun. Shufflenet v2: Practical guidelines for efficient cnn architecture design. *arXiv preprint arXiv:1807.11164*, 2018. [6](#)

[40] R. Miikkulainen, J. Liang, E. Meyerson, A. Rawal, D. Fink, O. Francon, B. Raju, H. Shahrzad, A. Navruzyan, N. Duffy, et al. Evolving deep neural networks. *arXiv preprint arXiv:1703.00548*, 2017. [1](#), [2](#)

[41] G. F. Miller, P. M. Todd, and S. U. Hegde. Designing neural networks using genetic algorithms. In *ICGA*, volume 89, pages 379–384, 1989. [1](#), [2](#)

[42] O. Nachum, M. Norouzi, and D. Schuurmans. Improving policy gradient by exploring under-appreciated rewards. *arXiv preprint arXiv:1611.09321*, 2016. [2](#)

[43] R. Negrinho and G. Gordon. Deeparchitect: Automatically designing and training deep architectures. *arXiv preprint arXiv:1704.08792*, 2017. [1](#), [2](#)

[44] H. Pham, M. Guan, B. Zoph, Q. V. Le, and J. Dean. Faster discovery of neural architectures by searching for paths in a large model. 2018. [3](#)

[45] H. Pham, M. Y. Guan, B. Zoph, Q. V. Le, and J. Dean. Efficient neural architecture search via parameter sharing. *arXiv preprint arXiv:1802.03268*, 2018. [6](#)

[46] E. Real, A. Aggarwal, Y. Huang, and Q. V. Le. Regularized evolution for image classifier architecture search. *arXiv preprint arXiv:1802.01548*, 2018. [1](#), [2](#), [6](#)

[47] E. Real, S. Moore, A. Selle, S. Saxena, Y. L. Suematsu, J. Tan, Q. Le, and A. Kurakin. Large-Scale Evolution of Image Classifiers. 2017. [1](#), [2](#)

[48] J. Schulman, F. Wolski, P. Dhariwal, A. Radford, and O. Klimov. Proximal policy optimization algorithms. *arXiv preprint arXiv:1707.06347*, 2017. [2](#)

[49] D. Silver, A. Huang, C. J. Maddison, A. Guez, L. Sifre, G. Van Den Driessche, J. Schrittwieser, I. Antonoglou, V. Panneershelvam, M. Lanctot, et al. Mastering the game of go with deep neural networks and tree search. *nature*, 529(7587):484–489, 2016. [1](#), [5](#)

[50] J. Snoek, H. Larochelle, and R. P. Adams. Practical bayesian optimization of machine learning algorithms. In *Advances in neural information processing systems*, pages 2951–2959, 2012. [2](#)

[51] K. O. Stanley. Compositional pattern producing networks: A novel abstraction of development. *Genetic programming and evolvable machines*, 8(2):131–162, 2007. [1](#), [2](#)

[52] K. O. Stanley, D. B. D’Ambrosio, and J. Gauci. A hypercube-based encoding for evolving large-scale neural networks. *Artificial life*, 15(2):185–212, 2009. [1](#)

[53] K. O. Stanley and R. Miikkulainen. Evolving neural networks through augmenting topologies. *Evolutionary computation*, 10(2):99–127, 2002. [1](#), [2](#)

[54] M. Suganuma, S. Shirakawa, and T. Nagao. A Genetic Programming Approach to Designing Convolutional Neural Network Architectures. 2017. [1](#), [2](#)

[55] R. S. Sutton, H. R. Maei, and C. Szepesvári. A convergent $o(n)$ temporal-difference algorithm for off-policy learning with linear function approximation. In *Advances in neural information processing systems*, pages 1609–1616, 2009. [2](#)

[56] C. Szegedy, V. Vanhoucke, S. Ioffe, J. Shlens, and Z. Wojna. Rethinking the inception architecture for computer vision. *CoRR*, abs/1512.00567, 2015. [13](#)

[57] C. Thornton, F. Hutter, H. H. Hoos, and K. Leyton-Brown. Auto-weka: Combined selection and hyperparameter optimization of classification algorithms. In *Proceedings of the 19th ACM SIGKDD international conference on Knowledge discovery and data mining*, pages 847–855. ACM, 2013. [2](#)

[58] M. Wistuba. Finding competitive network architectures within a day using uct. *arXiv preprint arXiv:1712.07420*, 2017. [1](#), [2](#)

[59] L. Xie and A. Yuille. Genetic cnn. *arXiv preprint arXiv:1703.01513*, 2017. [1](#), [2](#)

[60] S. Xie, R. Girshick, P. Dollár, Z. Tu, and K. He. Aggregated residual transformations for deep neural networks. In *Computer Vision and Pattern Recognition (CVPR), 2017 IEEE Conference on*, pages 5987–5995. IEEE, 2017. [6](#)

[61] K. Xu, J. Ba, R. Kiros, K. Cho, A. Courville, R. Salakhudinov, R. Zemel, and Y. Bengio. Show, attend and tell: Neural image caption generation with visual attention. In *International conference on machine learning*, pages 2048–2057, 2015. [9](#)

[62] K. Yoshizoe, A. Kishimoto, T. Kaneko, H. Yoshimoto, and Y. Ishikawa. Scalable distributed monte-carlo tree search. In *Fourth Annual Symposium on Combinatorial Search*, 2011. [5](#)

[63] B. Zoph and Q. V. Le. Neural Architecture Search with Reinforcement Learning. pages 1–16, 2016. [1](#), [2](#), [6](#)

[64] B. Zoph, V. Vasudevan, J. Shlens, and Q. V. Le. Learning transferable architectures for scalable image recognition. *arXiv preprint arXiv:1707.07012*, 2017. 3, 6, 7, 13

7. Pseudocode for AlphaX

In this section, we describe the pseudocode of the Distributed AlphaX. Algorithm 3 describes the search engine of AlphaX. Algorithm 2 is the server procedure to send the architecture to train chosen by the MCTS to the client and collect the architectures trained and their scores. Algorithm 1 is the client which trains and tests the architecture provided by the server.

Algorithm 1 Client

```

1: Require: Start working once building connection to the
   server
2: while True do
3:   if The client is connected to server then
4:      $network \leftarrow \text{Receive}()$ 
5:      $accuracy \leftarrow \text{Train}(network)$ 
6:     Send  $(network, accuracy)$  to the Server
7:   else
8:     Wait for re-connection
9:   end if
10:  end while

```

Algorithm 2 Server

```

1: while  $\text{size}(\text{TASK\_QUEUE}) > 2$  do
2:   while no idle client do
3:     Continue  $\triangleright$  Wait for dispatching jobs until there
   are idle clients
4:   end while
5:   Create a new connection to a random idle client
6:    $network \leftarrow \text{TASK\_QUEUE.pop}()$ 
7:   Send  $network$  to a Client
8:   if Received_Signal() then
9:      $network, accuracy \leftarrow \text{Receive\_Result}()$ 
10:     $acc(network) \leftarrow accuracy$ 
11:     $state \leftarrow \text{rollout\_from}(network)$ 
12:    Backpropagation( $state, (accuracy - \hat{q}(state))/2, 0$ )
         $\triangleright$  Replace  $\hat{q}$  with  $q = Q(s, a)$  in Eq. 2
13:    Train the meta-DNN with a new data
         $(network, accuracy)$ 
14:   else
15:     Continue
16:   end if
17: end while

```

Algorithm 3 Search Engine (MCTS)

```

1: function Expansion(state)
2:   Create a new node in a tree for state.
3:   for all action available at state do
4:      $Q(\text{state}, \text{action}) \leftarrow 0, \quad N(\text{state}, \text{action}) \leftarrow 0$ 
5:   end for
6: end function
7:
8: function Simulation(state)
9:   action  $\leftarrow$  none
10:  while action is not term do
11:    randomly generate an action
12:    next\_net  $\leftarrow$  Apply(state, action)
13:  end while
14: end function
15:
16: function Backpropagation(state, q, n)
17:   while state is not root do
18:     state  $\leftarrow$  parent(state)
19:      $Q(\text{state}, \text{action}) \leftarrow Q(\text{state}, \text{action}) + q$ 
20:      $N(\text{state}, \text{action}) \leftarrow N(\text{state}, \text{action}) + n$ 
21:   end while
22: end function
23:
24: Require: Start from the root
25: while episode  $< MAX\_episode do
26:   Server()
27:   cur\_state  $\leftarrow$  root\_node
28:   i  $\leftarrow 0$ 
29:   while i  $< MAX\_tree\_depth do
30:     i  $\leftarrow i + 1$ 
31:     next\_action  $\leftarrow$  Selection(cur\_state)  $\triangleright$  Select
32:     an action based on Eq. 1
33:     if next\_state not in tree then
34:       next\_state  $\leftarrow$  Expansion(next\_action)
35:       T  $\leftarrow$  Simulationt(next\_state) for t = 0...k
36:       T  $\leftarrow$  TASK_QUEUE.push(T)
37:        $\hat{q}(\text{next\_state}) \leftarrow \frac{1}{k} \sum_{i=1..k} \text{Pred}(\text{Ti})$ 
38:       Backpropagation(next\_state,  $\hat{q}$ )
39:       Preemptive backpropagation to send  $\hat{q}$ 
40:     end if
41:   end while
42: end while$$ 
```

\triangleright *Apply* returns the next state when action is applied to state

\triangleright *select* an action based on Eq. 1

\triangleright *k* is the number of simulations we run using the Meta-DNN

\triangleright *Pred* returns an accuracy predicted by the Meta-DNN

\triangleright *Backpropagation*(*next_state*, \hat{q})

\triangleright Preemptive backpropagation to send \hat{q}

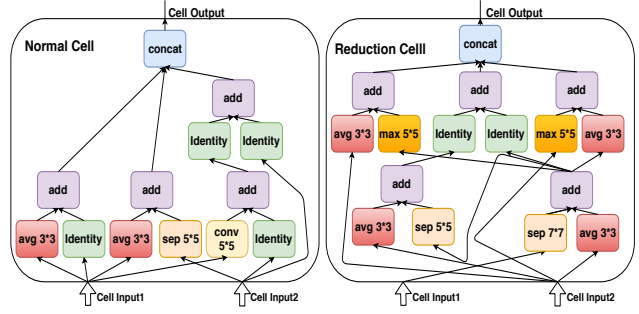


Figure 14: the *RCell* and *NCell* of AlphaX-2

8. Details of the State and Action Space

This section contains the description of the state and action space for NASNet design space.

We constrain the state space to make the design problem manageable. The state space exponentially grows with the depth: a k layers linear network has n^k architecture variations, where n is the number of layer types. We leverage the GPU DRAM size, our current computing resources and the design heuristics from leading DNNs, to propose the following constraints on the state space: 1) a branch has at most 1 layer; 2) a cell has at most 5 blocks; 3) the depth of blocks is limited to 2; 5) we use the layers in TABLE.3:

Actions also preserve the constraints imposed on the state space. If the next state reaches out of the design boundary, the agent automatically removes the action from the action set. For example, we exclude the "adding a new layer" action for a branch if it already has 1 layer. So, the action set is dynamically changing w.r.t states.

9. Experimental Setup for Section 5.3

The state space we consider consists of small simple CNNs. We consider a convolution layer and a softmax layer. For a convolutional layer, we allow a range of 1 or 2 for stride, 32 or 64 for filters, and 2 or 4 for kernels. We set the maximum depth to 3. We constraint that the final layer is always a dense layer with output size set to the number of classes.

Actions consist of (1) add conv layer, (2) add softmax layer, (3) increment or decrement one of the parameters for a convolution layer in the current CNN. For MCTS, random, and Q-learning agents have a terminal action to terminate the episode.

MCTS with meta-DNN: We implemented MCTS search algorithm followed the procedure with 4.2. c from Eq.1 is set to 200. The design of meta-DNN is consistent with 4.3. The meta-DNN model uses SGD optimizer with 0.9 momentum rate. All parameters in convolution layers are initialized with the random distribution. The learning rate

Table 3: The code of different types of layers

layers	code	layer	code	layer	code	layer	code
3x3 avg pool	1	3x3 max pool	4	3x3 conv	7	3x3 depth-separable conv	10
5x5 avg pool	2	5x5 max pool	5	5x5 conv	8	5x5 depth-separable conv	11
7x7 avg pool	3	7x7 max pool	6	identity	9	7x7 depth-separable conv	12

is set to 0.0001.

MCTS without meta-DNN: we also present the results without meta-DNN, the experiment setup is consistent with above but without meta-DNN assisted simulation.

Random: agent selects action uniformly at random.

Q-learning: We implemented a tabular Q-learning agent with ϵ -greedy strategy. The learning rate is set to 0.2. We set the discount factor to be 1 in order not to prioritize short-term rewards. We fix ϵ to 0.2. We initialize the Q-value with 0.5.

Hill Climbing: For a hill climbing, an agent starts from a randomly chosen initial state. It trains every architecture in the child nodes and moves to the child node of which architecture performed the best, and repeat this procedure. Unlike MCTS and Q-learning which trains a NN only when it is a terminal state, hill climbing considers every state (and its child nodes) it visits to train. As such, we do not have a terminal action for hill climbing. As we observed that the hill climbing tends to stick to a local optimum, we restart from a randomly chosen initial state if it visits the same state twice in the trajectory.

10. Experiment Setup for Searching and Training

10.1. Setup for searching networks on CIFAR

We use 16 NV-1080ti gpus for searching procedure. One of them is the server running the searching program and remaining 15 gpus are clients for training the searched architectures. We use dictionary data structure in Python to save the searched architectures and convert to json file to store them in the disk. All of our training procedures are implemented in MXNET framework. The setup for training CIFAR-10 during the search are as follows: 1) we early terminate the training at the 70th epoch(3 periods of cosine restart learning rate schedule[38]) due to the limited computing resources; then we rank networks to filter out top ones to perform additional 560 epochs to acquire the final accuracy. 2) cutout is applied [64] by using 1 crop of size 16×16 . 3) Our models use cosine restart learning rate schedule[38] with 3 periods, the base learning rate is 0.05 and the batch size is 144. 4) We use the momentum optimizer with momentum rate set to 0.9 and L2 weight decay. 5) We also use dropout ratio schedule in the training. The droppath ratio is set to 0.3 and dense dropout ratio is set to 0.2 for searching procedure and applied *Schedule*-

DropPath[64] for the final training. 6) We use an auxiliary classifier located at 2/3 of depth of the network. The loss of the auxiliary classifier is weighted by 0.4[56]. 7) The weights of our models are initialized with Gaussian distribution subjected to 0.01 standard deviation. 8) we randomly crop 32×32 patches from upsampled images of size 40×40 and apply random horizontal flips consistent with[64].

10.2. Setup for ImageNet

The setup for training ImageNet are as follows: 1) we construct the network for ImageNet with searched *RCell* and *NCell* according to Fig.7 in [64]. 2) the input image size is 224×224 (the mobile setting across literature). 3) Our models for ImageNet use polynomial learning rate schedule, starting with 0.05 and decay through 200 epochs. 4) We use the momentum optimizer with momentum rate set to 0.9 and L2 weight decay. 5) Our model uses an auxiliary classifier located at 2/3 of depth of the network. The loss of the auxiliary classifier is weighted by 0.4[56]. 6) Dense dropout is applied to the final softmax layer with probability 0.5. 7) We set the batch size as 256. 8) The weights of our models are initialized with Gaussian distribution subjected to 0.01 standard deviation.

11. Setup for Vision Models

11.1. Object detection

We use AlphaX-1 model pre-trained on ImageNet dataset. The training dataset is MSCOCO for object detection[30] which contains 90 classes of objects. Each image is scaled to 300×300 in RGB channels. We trained the model with 200k iterations with 0.04 initial learning rate and the batch size is set to 24. We applied the exponential learning rate decay schedule with the 0.95 decay factor. Our model uses momentum optimizer with momentum rate set to 0.9. We also use the L2 weight decay for training. We process each image with random horizontal flip and random crop[37]. We set the matched threshold to 0.5, which means only the probability of an object over 0.5 is effective to appear on the image. We use 8000 subsets of validation images in MSCOCO validation set and report the mean average precision (mAP) as computed with the standard COCO metric library[31].

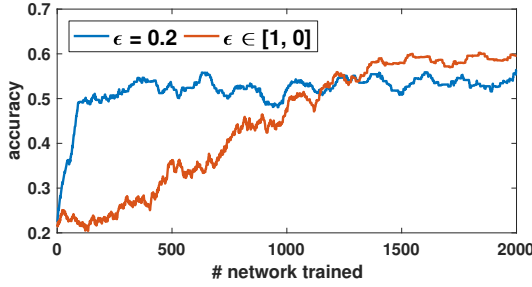


Figure 15: The effect of ϵ toward the top accuracy in the search.

11.2. Neural style

We implement the neural style transfer application by replacing the VGG model to AlphaX-1 model[18]. AlphaX-1 model is pre-trained on ImageNet dataset. In order to produce a nice result, we set the total 1000 iterations with 0.1 learning rate. We set 10 as the style weight which represents the extent of style reconstruction and 0.025 as the content weight which represents the extent of content reconstruction. We test different kinds of combinations of the outputs of different layers. Fig.16 shows the structure of AlphaX model, we found that for AlphaX-1 model, the best result can be generated by the concat layer of 13th normal cell as the feature for content reconstruction and the concat layer in first reduction cell as the feature for style reconstruction, the types of layers in each cell are shown in Fig.7 and Fig.14.

11.3. Image captioning

The training dataset of image captioning is MSCOCO[30], a large-scale dataset for the object detection, segmentation, and captioning. Each image is scaled to 224×224 in RGB channels and subtract the channel means as the input to a AlphaX-1 model. For training AlphaX-1 model, We use the SGD optimizer with the 16 batch size and the initial learning rate is 2.0. We applied the exponential learning rate decay schedule with the 0.5 decay factor in every 8 epochs.

12. ϵ Scheduling for Q-Learning

In this section, we investigate the effect of the hyper-parameter ϵ on the performance of Q-learning. Fig.15 is the comparison of Q-learning with two configurations of ϵ . $\epsilon \in [1, 0]$ means we reduce ϵ by 0.1 every 200 steps. Here, we try to find a linear network with a depth up to 10.

We observed that a small ϵ (encouraging exploitation) quickly converges to a local optimal; a large ϵ (encouraging exploration), though slow, finds networks with higher accuracies. This suggests that the performance of Q-learning is contingent on choosing a good scheduling of the hyper-parameter ϵ . Baker et al. [5] proposed to start Q-learning

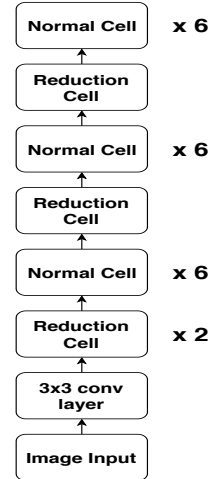


Figure 16: Cell based architecture of AlphaX model

with the exploration probability (ϵ) set to 1.0, gradually reducing the ϵ down. While Q-learning requires to manually tune the schedule of the probability of exploration, the upper confidence bound in MCTS automatically balances the exploration and exploitation based on the number of visits (Fig.1) and only requires to choose a single parameter c . Because our goal is to minimize the amount of human effort required for deep learning, we deployed UCT for our search engine.